

AD-A139 191

OPTICAL IMAGING OF A COUPLING REGION BETWEEN
INTER-STREAMING PLASMAS(U) NAVAL RESEARCH LAB
WASHINGTON DC J A STAMPER ET AL. 24 FEB 84

NRL-MR-5278

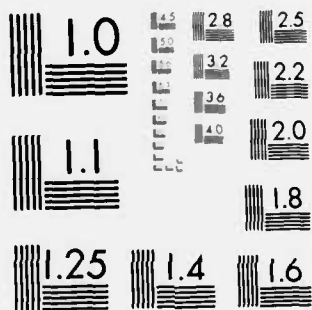
1/1

UNCLASSIFIED

F/G 20/6

NL





MICROCOPY RESOLUTION TEST CHART
NATIONAL BUREAU OF STANDARDS-1963-A

AD A139191

NRL Memorandum Report 5278

Optical Imaging of a Coupling Region Between Inter-Streaming Plasmas

J. A. STAMPER, B. H. RIPIN, E. A. MCLEAN,
AND S. P. OBENSCHAIN

*Laser Plasma Branch
Plasma Physics Division*

February 24, 1984

This research was sponsored by the Defense Nuclear Agency under Subtask I25BMXIO,
work unit 00024 and work unit title "Early Time Plasma."



DTIC
ELECTE
MAR 21 1984
S
A

NAVAL RESEARCH LABORATORY
Washington, D.C.

Approved for public release; distribution unlimited.

DTIC FILE COPY

84 03 21 075

SECURITY CLASSIFICATION OF THIS PAGE

AD-A131191

REPORT DOCUMENTATION PAGE				
1a. REPORT SECURITY CLASSIFICATION UNCLASSIFIED		1b. RESTRICTIVE MARKINGS		
2a. SECURITY CLASSIFICATION AUTHORITY		3. DISTRIBUTION/AVAILABILITY OF REPORT		
2b. DECLASSIFICATION/DOWNGRADING SCHEDULE		Approved for public release; distribution unlimited.		
4. PERFORMING ORGANIZATION REPORT NUMBER(S) NRL Memorandum Report 5278		5. MONITORING ORGANIZATION REPORT NUMBER(S)		
6a. NAME OF PERFORMING ORGANIZATION Naval Research Laboratory	6b. OFFICE SYMBOL (If applicable)	7a. NAME OF MONITORING ORGANIZATION		
6c. ADDRESS (City, State and ZIP Code) Washington, DC 20375		7b. ADDRESS (City, State and ZIP Code)		
8a. NAME OF FUNDING/SPONSORING ORGANIZATION Defense Nuclear Agency	8b. OFFICE SYMBOL (If applicable)	9. PROCUREMENT INSTRUMENT IDENTIFICATION NUMBER		
8c. ADDRESS (City, State and ZIP Code) Washington, DC 20305		10. SOURCE OF FUNDING NOS.		
		PROGRAM ELEMENT NO.	PROJECT NO.	TASK NO.
		62715H		47-1606-0-4
11. TITLE (Include Security Classification) (See page ii)				
12. PERSONAL AUTHOR(S) J.A. Stamper, B.H. Ripin, E.A. McLean, and S.P. Obenschain				
13a. TYPE OF REPORT Interim	13b. TIME COVERED FROM _____ TO _____	14. DATE OF REPORT (Yr., Mo., Day) February 24, 1984	15. PAGE COUNT 31	
16. SUPPLEMENTARY NOTATION This research was sponsored by the Defense Nuclear Agency under Subtask I25BMXIO, work unit 00024 and work unit title "Early Time Plasma."				
17. COSATI CODES		18. SUBJECT TERMS (Continue on reverse if necessary and identify by block number)		
FIELD	GROUP	SUB. GR.		
		Plasma		
		Coupling		
		Inter-streaming		
		Optical imaging		
19. ABSTRACT (Continue on reverse if necessary and identify by block number)				
<p>Recent studies in the NRL HANE simulation experiment have been directed toward a higher pressure/low altitude regime where HANE events (e.g., Checkmate) and early HANE simulations ($P \geq .5$ Torr) had shown a turbulence or jetting. The main diagnostic was dual-time, dark-field shadowgraphy which had sufficient temporal (300 psec) and spatial (10 micron) resolution to resolve details of the developing structure. A well-defined, initially nearly-spherical front or coupling region is seen which slows down, indicating mass pick-up. At higher ambient pressure, lower laser energy and later time, the front shows a breakup. When conditions are just marginal for break-up, the front tends to form a single protuberance or aneurism which grows in time.</p>				
20. DISTRIBUTION/AVAILABILITY OF ABSTRACT UNCLASSIFIED/UNLIMITED <input checked="" type="checkbox"/> SAME AS RPT. <input type="checkbox"/> DTIC USERS <input type="checkbox"/>		21. ABSTRACT SECURITY CLASSIFICATION UNCLASSIFIED		
22a. NAME OF RESPONSIBLE INDIVIDUAL J. A. Stamper		22b. TELEPHONE NUMBER (Include Area Code) (202) 767-2683	22c. OFFICE SYMBOL Code 4730	

DD FORM 1473, 83 APR

EDITION OF 1 JAN 73 IS OBSOLETE.

SECURITY CLASSIFICATION OF THIS PAGE

SECURITY CLASSIFICATION OF THIS PAGE

11. TITLE

OPTICAL IMAGING OF A COUPLING REGION BETWEEN INTER-STREAMING PLASMAS

SECURITY CLASSIFICATION OF THIS PAGE

CONTENTS

I. INTRODUCTION	1
II. EXPERIMENTAL BACKGROUND	2
III. EXPERIMENTAL STUDIES AND RESULTS	3
IV. CONCLUSION	8
ACKNOWLEDGMENTS	9
REFERENCES	19
APPENDIX: DENSITY ESTIMATE FROM REFRACTION	20

Accession For	
NTIS GRA&I	<input checked="checked" type="checkbox"/>
DTIC TAB	<input type="checkbox"/>
Unannounced	<input type="checkbox"/>
Justification	
By	
Distribution/	
Availability Codes	
Dist	Avail and/or Special
A-1	



OPTICAL IMAGING OF A COUPLING REGION BETWEEN INTER-STREAMING PLASMAS

I. INTRODUCTION

Our studies at higher ambient pressures ($> .2$ Torr) were aimed at understanding phenomena in HANE events at altitudes of 100 to 200 km. For example, jetting and a turbulent appearing coupling region were seen in Checkmate. The original^{1,2,3} NRL simulation experiment (~ 1970) had shown a turbulent appearing coupling region at higher ambient pressure ($> .5$ Torr) and helped to motivate the most recent (high-pressure) HANE studies. Our present (non-resonant) optical probing diagnostics are useful at these higher densities. We start with a brief review of the 1970 data.

Visualization of the coupling region between the expanding debris plasma and the ambient plasma has been an important objective of the HANE simulation experiments. This has been accomplished by either fast photography of the emitted light or by using a short-pulse probing laser beam. Fast framing photography in the 1970 NRL experiment showed a region of strong momentum coupling. Typically, 10 Joules of laser energy in a 30-45 nsec pulse was used to produce target debris (CH_2) which streamed into an ambient nitrogen gas at 0.1 to 1 Torr. The coupling region in the 1970 experiment was also imaged using second-harmonic shadowgraphy and was seen to develop a turbulent appearance at higher ($\geq .5$ Torr) pressure and at later times.

The time dependence of the coupling region is shown in Fig. 1 for an ambient nitrogen background gas at 200 mTorr. The coupling region was well formed by 53 nsec and was observed out to 92 nsec. These shadowgrams were taken in the second harmonic light (5320 Angstrom) of the main laser beam. Although the probe pulse was about 20 nsec in duration, a sweeping action gave an effective exposure of only a few nanoseconds.

Manuscript approved December 15, 1983.

The pressure dependence of the coupling region is shown in Fig. 2. These shadowgrams were all taken at 92 nsec and show the dependence on the pressure of an ambient nitrogen gas. Above about 500 mTorr the coupling region shows a turbulent appearance. This is the phenomena which we want to investigate in the present experiment. The coupling region observed in the original experiment showed a radius versus time dependence which agreed with a detonation wave at early times (during the main laser pulse) and with a blast wave at later times. This is illustrated in Fig. 3 for a 120 mTorr ambient gas pressure. In the present experiment, with a much shorter laser pulse, the blast-wave scaling is shown to apply over a large range of laser and ambient conditions.

II. EXPERIMENTAL BACKGROUND

Dark-field shadowgraphy is a very useful diagnostic of the high-pressure coupling fronts. In the present experiment, with a shorter (4 nsec) and more energetic (up to 160 Joules) main laser pulse than in the 1970 experiment, the luminous fronts observed with fast (framing) photography were not very well resolved. However, by using a very short (300 psec) probing laser pulse and dark-field shadowgraphy, we have been able to obtain high resolution (few micron), dual-time photographs of structure in the coupling region.

Dark-field shadowgraphy allows the preferential sampling of the steep-gradient region of an expanding plasma front and permits two-dimensional multiple-time recordings on a single photograph.⁴ The dark background also allows one to see faint luminous regions or regions of density variation (e.g., due to photoionization by front radiation) near the coupling region. The diagnostic is thus well suited for studying phenomena in and near the coupling region.

The experimental set-up is illustrated in Fig. 4. The second harmonic probing laser beam is incident from the right, parallel to the target surface.

A 25-cm focal length lens, positioned 50 cm from the target (for one-to-one imaging) is used to collect the light. Probe light that is not appreciably deflected by the plasma is focused by the lens, and blocked by a small opaque mask at its back focal plane. This produces a dark background. However, light that passes through the steep-gradient region (front) is deflected and then is redirected by the lens past the mask and recorded. Thus, a bright profile of the steep-gradient region is recorded on the dark background. The purpose of the mask can be described more quantitatively as filtering out the longer transverse spatial wavelengths. Thus, one records the shorter wavelengths or larger wavenumbers which characterize the steeper gradients.

On most of the shots, two delayed probing laser pulses were used and spaced in time to avoid image superposition. Thus, bright profiles of the coupling-front region were obtained at two times so that front deceleration and break-up evolution could be seen. The probe pulses at these two times were filtered with separate masks. The density of the scattering region was about four orders of magnitude below the critical density of the probing radiation resulting in refraction through very small angles ($\sim 10^{-4}$ radian). This placed a severe restriction on the spatial filtering so that the probe light focused onto the masks had to be placed very close (~ 100 micron) to the edge of the masks (typically around 1 mm dimension).

III. EXPERIMENTAL STUDIES AND RESULTS

Conditions for the dark-field shadowgraphy studies are summarized in Table I. Data was taken over a large range of laser and ambient gas parameters. The equal-mass coupling radius dependence on laser energy and ambient pressure was checked. The laser irradiance (and thus debris velocity) was varied (at a fixed laser energy) by varying the laser spot size. Although a few shots were taken

with an ambient magnetic field (0.63 kG), the coupling did not appear to be magnetic field dependent at the higher pressures ($> .2$ Torr) used in the dark-field study. Ripin et al.⁵ correlates these data using blast-wave model scaling. We concentrate here on discussing the general features of the coupling shells and the nonuniformities evolving from them.

Table 1 — Dark-field shadowgraphy studies

(VARIATIONS)

- o LASER ENERGY (4 TO 160 JOULES)
- o LASER SPOT SIZE (.25 MM OR 1 MM)
- o AMBIENT PRESSURE (.2 TO 10 TORR)
- o AMBIENT COMPOSITION (.9 N₂ + .1 H₂ OR HE)
- o AMBIENT MAGNETIC FIELD (0 OR .63 kG)

(SPECIAL TARGETS)

- o TARGET TILTED ABOUT HORIZONTAL AXIS
- o CH TARGETS WITH STRIPES (Al OR Au)

Some of the dependences and structures are presented in the next few figures. See Fig. 5 for example. The main laser beam is incident from the right. The distances can be judged from the 5 mm spacing in the target holder - seen on the left. The ambient gas was 90 percent nitrogen with 10 percent hydrogen (as a spectroscopic diagnostic). The targets were 4.6 micron-thick aluminum foils. The coupling regions (bright rings) are seen at two different times as they expand to the right. There is also a bright patch, due to probe light scattered by debris plasma near the target surface, or due to emitted light in the band pass of the filter on the left, just in front of the target surface. The bright, narrow, curved region of dense, ablatively accelerated target material is seen on the left, going to the left. Figure 5 (shot number 13672) shows the coupling region at 52 nsec and 164 nsec after the peak of the 20 Joule main laser pulse. In this case, the ambient nitrogen/hydrogen gas pressure was 1.5 Torr. One can see a nearly-spherical, sharply-defined coupling shell of thickness about 300 μm . Often the shell exhibits a thin dark region between two bright regions; this is expected when the shell is thin with steep gradients on the outer and inner surfaces. There is some evidence at the later time and larger radius that deviations from the smooth shell are developing. The exposure taken at 52 nsec shows a shell with a radius of curvature of 1 cm and with structure within the shell consistent with gradient scalelengths of only 10^{-2} cm. In order to obtain this exposure, it was necessary to have the focus of the collimated probe beam only 10^{-2} cm from the edge of the mask. Using this information and the 25-cm focal length of the lens, one can place a lower limit on the density sampled.

A method for estimating the minimum density consistent with the dark-field and shell parameters is outlined in the appendix. We note that the second-harmonic probe light must have been refracted in the front region by at least 10^{-2} cm/25 cm or by 4×10^{-4} rad in order to clear the mask and be recorded.

The angle of refraction θ is seen to depend on the gradient of the refraction index along the ray trajectory. For a fully-ionized plasma (where electron refractivity dominates) the index is shown in terms of the electron density n and critical density (10^{21} cm^{-3}) n_c at the main laser wavelength. Since refraction is weak one could take the path length d through the shell as the diameter of a chord with the penetration depth s related to d by the sagitta formula. If the penetration depth is about a gradient scalelength L , then n/n_c is of the order of $\sqrt{9L/2r}$. Alternatively, if we use Bouguer's relation, which is valid for spherical symmetry, we can express the refraction angle as an integral over radius and thus avoid the problems of working with an unknown ray trajectory. The density ratio n/n_c can then be expressed in terms of the closest point of approach a to the center of spherical symmetry and the impact parameter $b = a\bar{n}(a)$. For a thin shell, a is approximately r , the radius of curvature. For weak refraction by a thin shell, one can expand about the lower limit (a singularity) of the integral and choose an upper limit cut-off to get, $n/n_c \approx \sqrt{9L/2r}$. Since $\theta > 4 \times 10^{-4}$, we find $n > 10^{17} \text{ cm}^{-3}$. Actually, spectroscopy shows that the electron density in the shell is around 10^{18} cm^{-3} , which is substantially higher than our lower limit.

Returning now to a discussion of features observed under different experimental conditions, we consider a shot (number 13630) where the ambient pressure is increased to 3.2 Torr. See Fig. 6. Here, the energy in the main laser pulse was 46 Joules. The observation times were 52 and 96 nsec for this and the remaining shadowgrams. The deviation from spherical symmetry is now apparent. A single protuberance or aneurism is seen to be growing in time. The light-dark-light pattern is seen in both the initial shell and aneurism.

As the ambient pressure is increased still further to 5 Torr, as shown in Fig. 7, the aneurism is clearly developed, even at the earlier time (52 nsec).

For this shot (number 13621), an additional small aneurism is also seen developing at the base of the large aneurism. The energy of the main laser pulse was 38 Joules for this shot. An (out of focus) image of the magnetic induction coil is seen on the right. Possible mechanisms causing the aneurism and front break-up are discussed elsewhere.⁵⁻⁸ The deceleration of the front could play a role in the break-up mechanism. There is adequate time for the Rayleigh-Taylor instability to evolve, if present, although the development of a single protuberance and the growth of wavelengths so much greater than the front thickness is difficult to understand. Also, because of the heating and mass motion in the decelerating coupling region, free convection could play a role in the front break-up. A periodic structure along the front can be seen on this shot but contributions from the diagnostic cannot be ruled out.

As the laser energy is lowered to 8.6 Joules at the 5 Torr pressure, the front break-up starts to show a more complicated structure as is seen in Fig. 8 for shot number 13642. When the laser energy is lowered still further to 4.1 Joules, as shown in Fig. 9 for shot number 13641, the front shows multiple break-up. The special targets, mentioned in Table I, were also used to provide additional information on the aneurisms. In order to check whether the aneurism is related to the incident laser path, the target was tilted about 15 degrees about a horizontal axis on shot number 13684. The aneurisms appeared in a position more along the target normal than the direction of the incident laser. We also tried to induce aneurisms by using structured targets. A target with 50 micron wide aluminum stripes and a 50 micron spacing on a CH plastic film support was used on shot number 13658. Although about 3 stripes were in the focal region, the aneurisms were only seen in the central region of the front. However, a similar shot (number 13683) with gold stripes (instead of aluminum, which produced larger Z/A variations across the target surface) did

show some aneurisms forming to either side of the central region. This provides some evidence that the aneurisms can be seeded in the target structure.

Another feature, observed on a few shots, was a faint secondary front located just outside of the main front. A disturbed region ahead of the main front could be produced by light emitted from the front or by heat conducted from the front. In this case, the observed image is probably due to probe light being refracted by a gentle (weaker than the shock front) density gradient. Emitted light from the outside region is not a likely contributor since it would be smeared by the motion of this region, whereas the observed secondary fronts appear well resolved.

IV. CONCLUSION

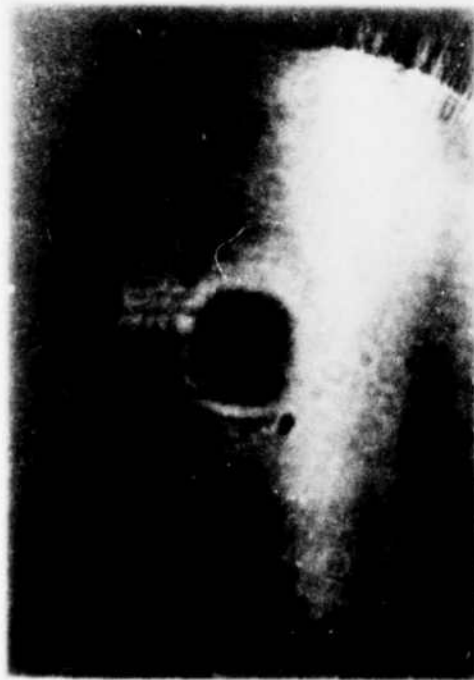
In summary, there are several features that can be easily seen in the dark-field shadowgrams: (1) There is a well-defined, thin, nearly-spherical front or coupling region that is slowing down, indicating mass pick-up, (2) Under some conditions (higher pressure, lower energy and later time) the front shows break-up, or marked departure from a spherical shape, (3) When conditions are just marginal for break-up, the front tends to form a single protuberance or aneurism which grows in time, (4) Further into the unstable region, the front shows multiple break-up, (5) Periodic structure is sometimes seen along the front, and (6) On some shots, a fainter secondary front is sometimes seen ahead of the main coupling region.

Finally, we point out some further areas of promising optical diagnostic development for the NRL HANE simulation. These include: (1) Resonant scattering with a dye laser tuned to an ion resonance. This will extend the studies to lower density and allow us to carry out species-specific scattering. We could, for example, scatter off of particular debris or ambient ions, (2) Imaging the Fourier-Transform plane will allow us to record the

angular scatter of a probe light passing through various structures. This would allow a measure of the plasma power function $P(\omega, k)$. (3) Dark-field shadowgraphy is one example of spatial filtering in the Fourier-Transform plane. There are other selective filter schemes which we could consider. (4) We could utilize the polarizations of scattered probe light to obtain information about structures aligned along the magnetic field or, if the field is large enough, measure the magnetic field itself with Faraday rotation. (5) A longer wavelength laser could be considered for several optical diagnostics of lower density phenomena, and (6) Optical diagnostics being developed to study the Rayleigh-Taylor instability in the ablatively accelerated targets will give information on the disassembly phase.⁹ For example, the angular pattern of light scattered, at a steep angle of incidence, from the heated side of the target gives information on a high-density (for optical probing) periodic structure.

ACKNOWLEDGMENTS

This work was supported by the Defense Nuclear Agency.



12 nsec



23 nsec



53 nsec



98 nsec

200 mT

R-1021

Fig. 1 — Original NRL/HANE Experiment: Single-time, bright-field shadowgrams showing the temporal variation of the coupling region or shock for an ambient nitrogen gas at 200 mTorr.



200 mT



500 mT



750 mT



1000 mT

R-1022

$t = 92 \text{ nsec}$

Fig. 2 — Original NRL/HANE Experiment: Shadowgrams showing the pressure dependence of the coupling region at 92 nsec. Above about 500 mTorr, the coupling region shows a turbulent appearance.

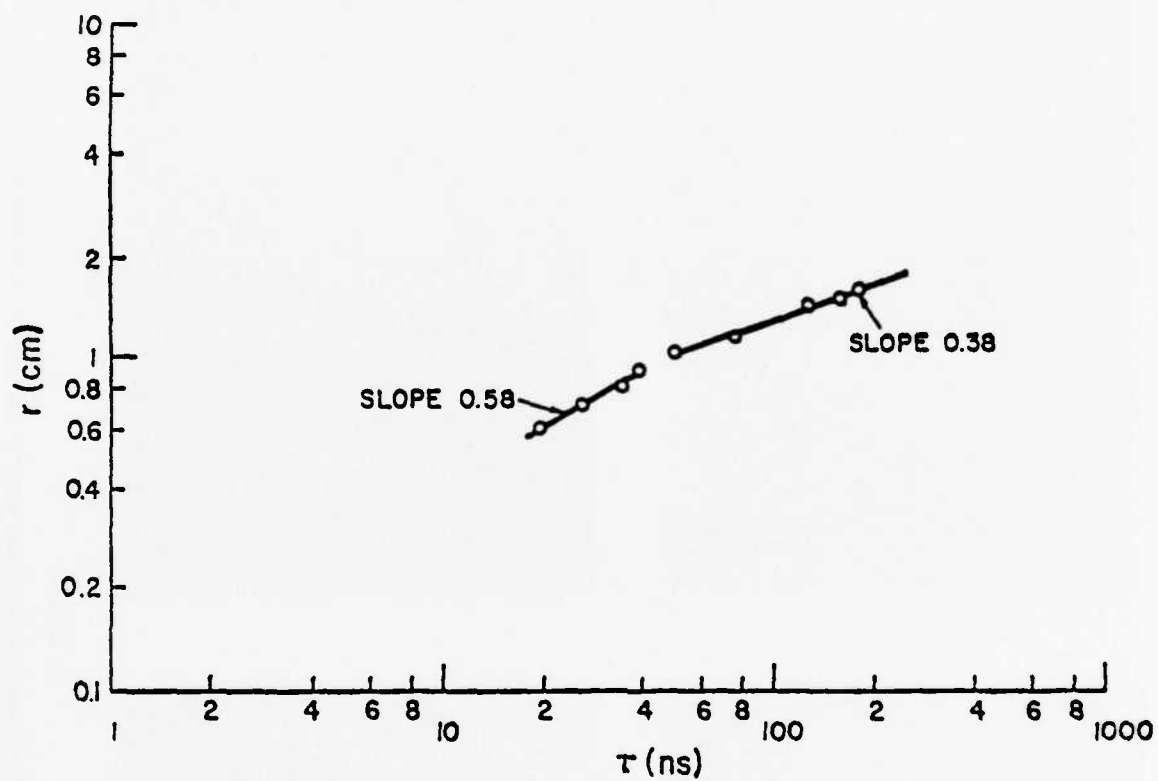


Fig. 3 — Original NRL/HANE Experiment: Radius of coupling region versus time for shots in a 120 mTorr ambient nitrogen gas. The variation follows that of a detonation wave at early times (during the main laser pulse) and follows that of a blast wave at late times.

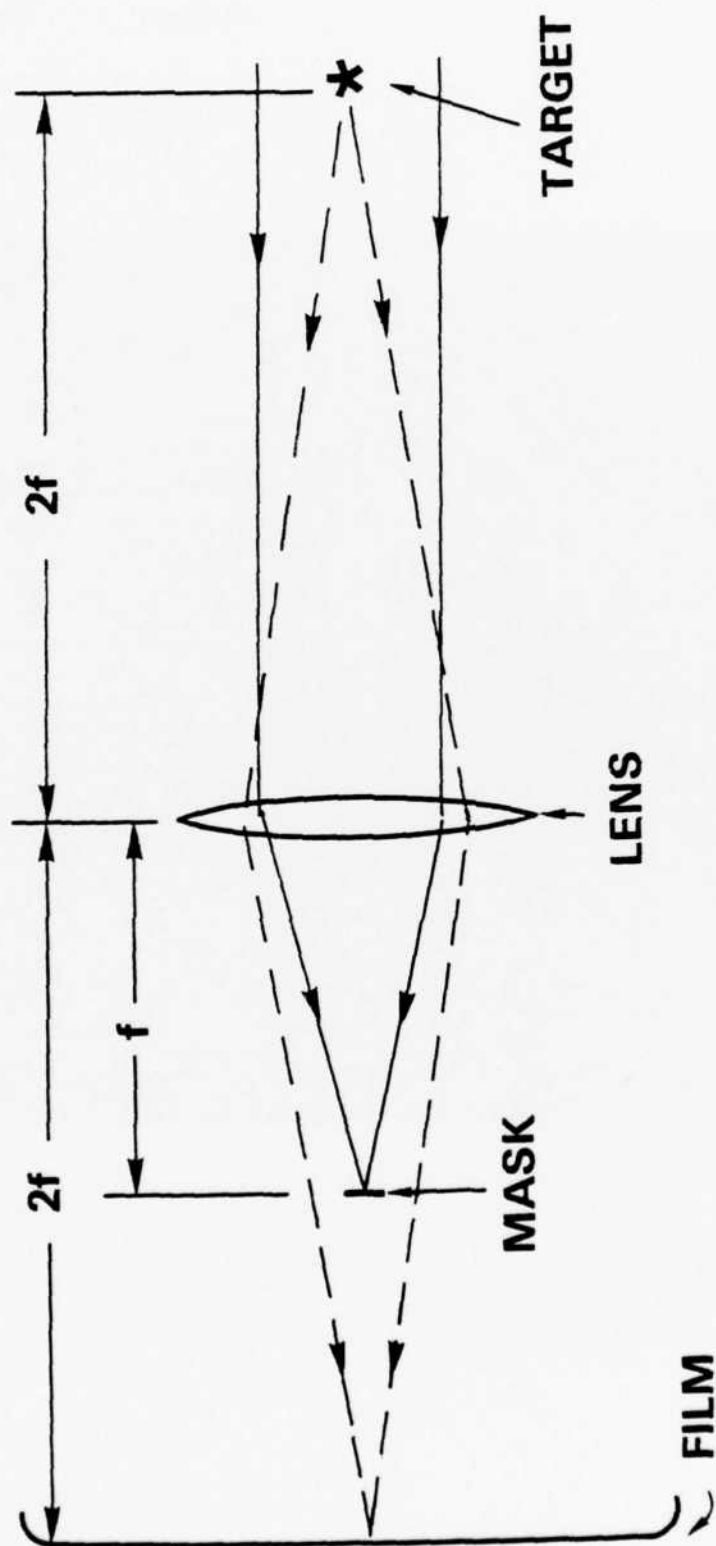
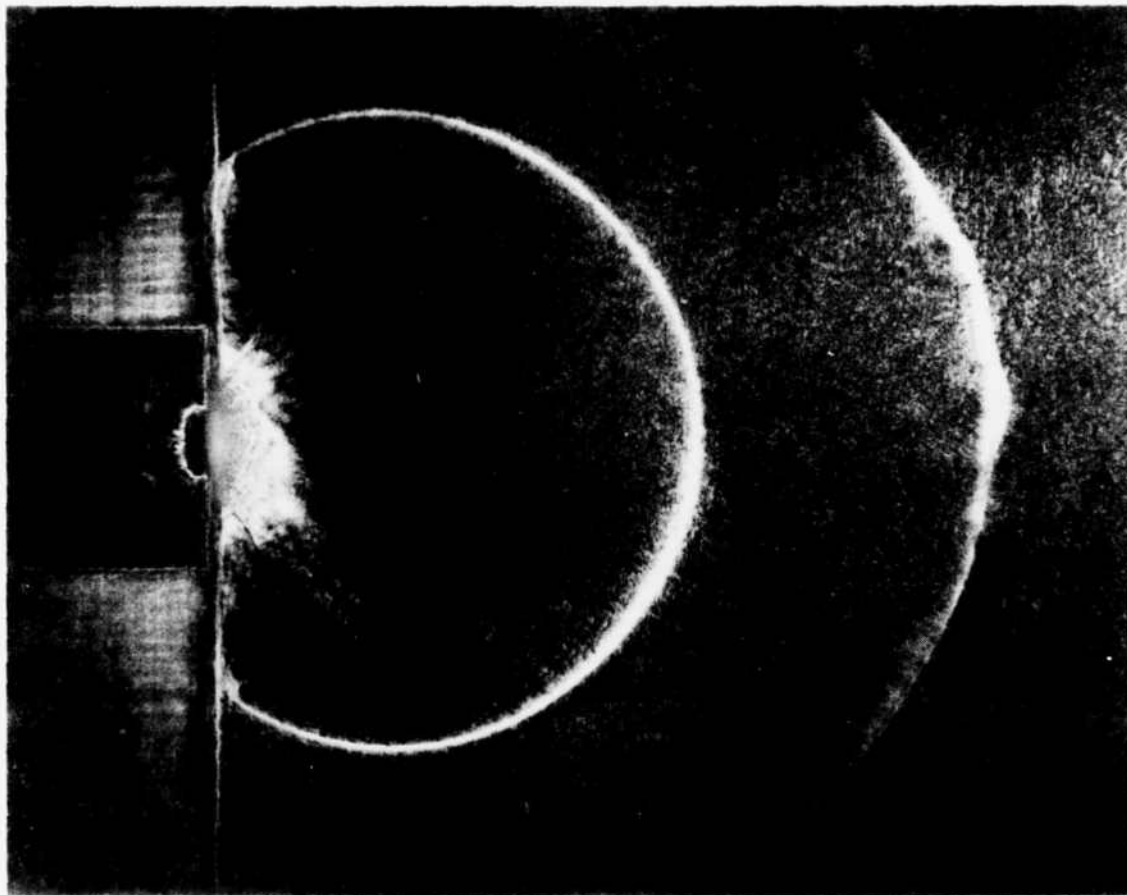
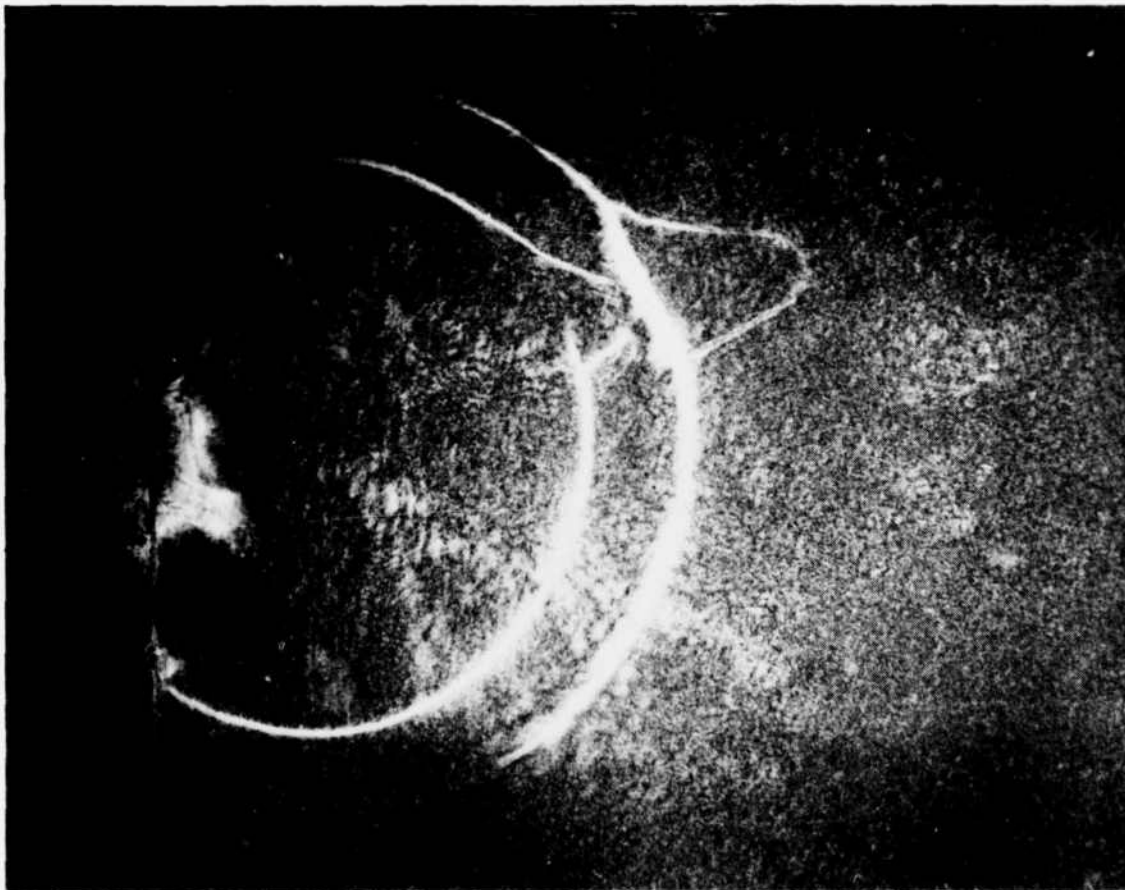


Fig. 4 -- Experimental arrangement for dark-field shadowgraphy in the present NRL/JHANE experiment.
A 300 psec (FWHM) second-harmonic (5270 Å) laser probe was used.



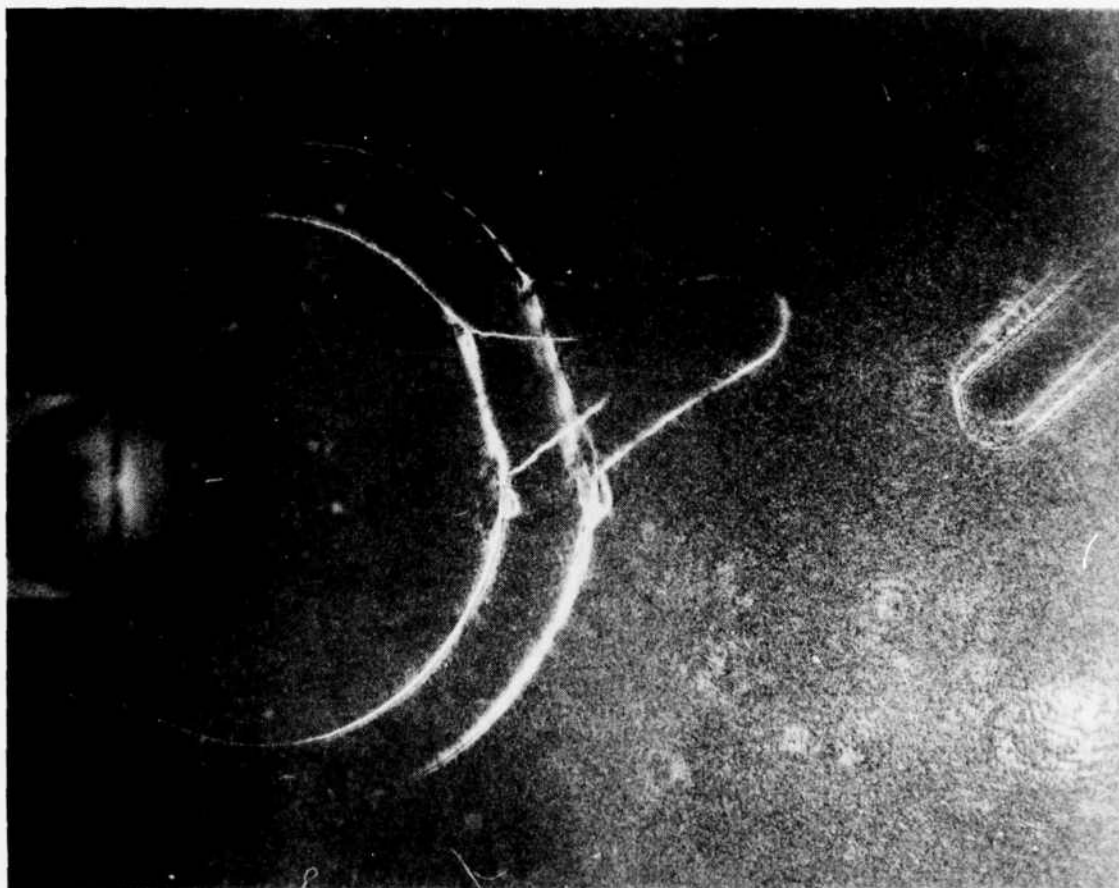
R-1023

Fig. 5 — Dual-time, dark-field shadowgram of a shock front in a 1.5 Torr (90% N₂ + 10% H₂) gas. The observation times were 52 nsec and 164 nsec, the incident laser energy was 20 J, and a 630 gauss magnetic field was present, into the plane of the paper. The shock (coupling region) is seen (at the two times) as the two, thin, large, bright, nearly-circular regions on the right. The smaller, broad, bright region in the right near the initial target is probably due to probe light scattered by slow-moving debris plasma. A smaller, thin, irregular bright region of ablatively-accelerated dense target material is seen on the left. Sizes can be judged by the approximately 5 mm gap in the target holder. Shot number was 13672.



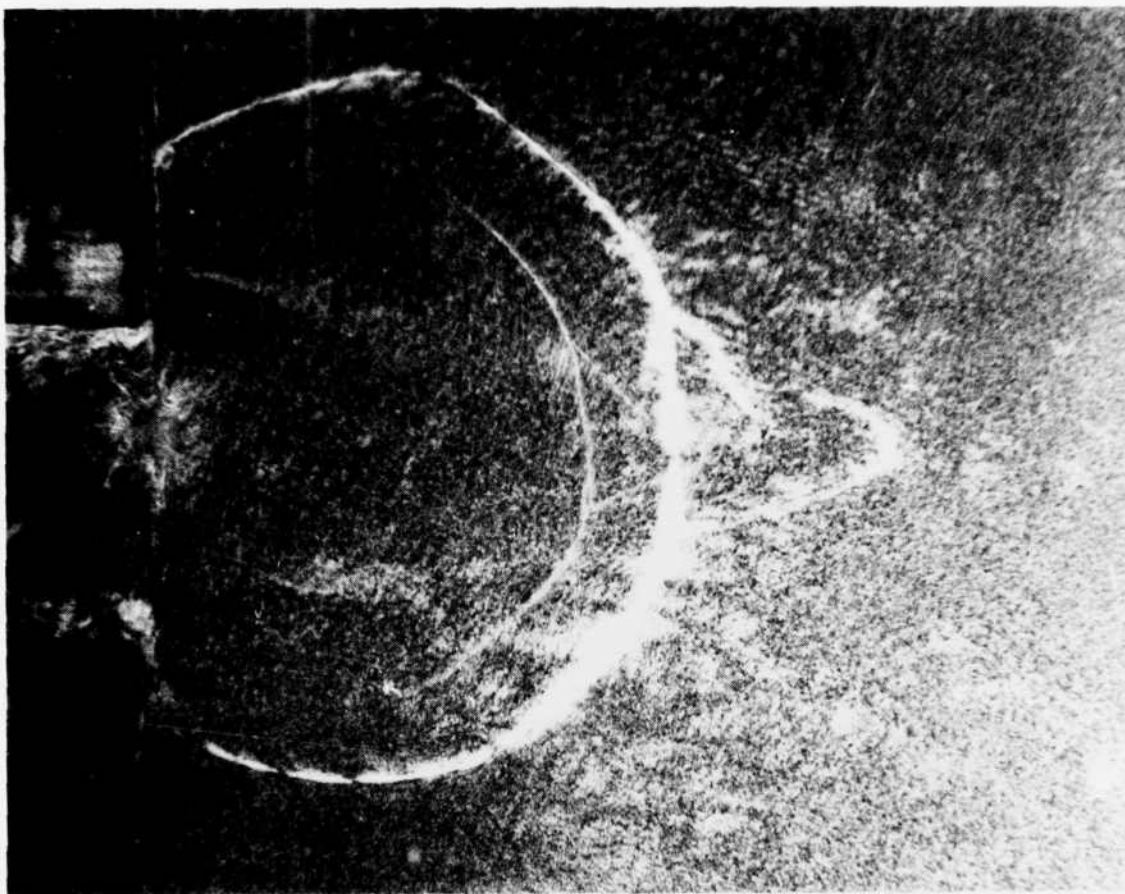
R-1026

Fig. 6 — Shadowgram of a shock front in a 3.25 Torr (N₂,H₂) gas. The laser energy was 46 J and the times were 52 and 96 nsec. A single protuberance or aneurism is seen, growing in time. Shot number was 13630.



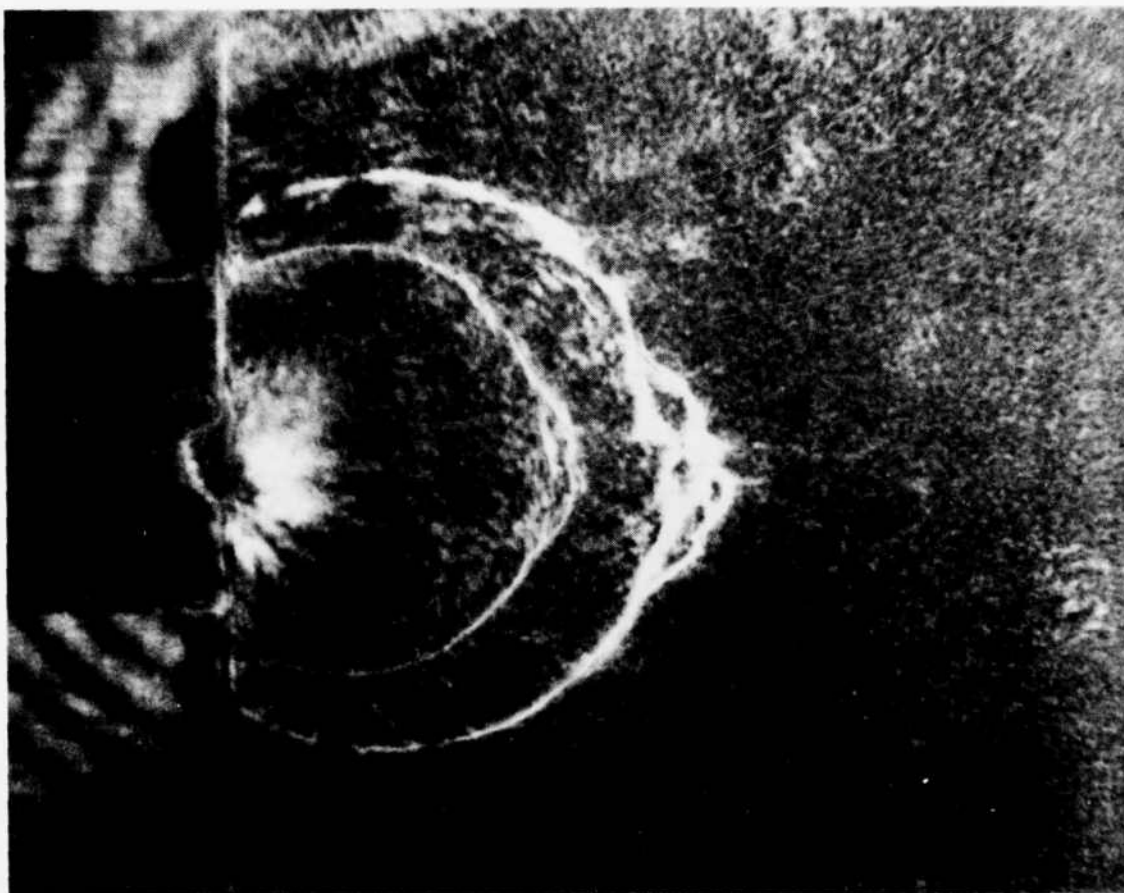
R 1025

Fig. 7 — Shadowgram of a shock front in a 5.0 Torr (N₂,H₂) gas. The laser energy was 38 J and the times were 52 and 96 nsec. The aneurism is clearly developed, even at 52 nsec. Note, the additional, small aneurism developing at the base of the large aneurism. Shot number was 13621.



R-1027

Fig. 8 — Shadowgram of a shock front in a 5.0 Torr (N₂,H₂) gas with less (8.6 J) laser energy on target. Times were 52 and 96 nsec. The aneurism shows a more complicated structure. Shot number was 13642.



R-1024

Fig. 9 — Shadowgram of a shock front in a 5.0 Torr (N_2H_2) gas with still less (4.1 J) laser energy on target. Times were 52 and 96 nsec. Note the complicated shock break-up, showing the growth of multiple aneurisms. Shot number was 13641.

REFERENCES

1. J.A. Stamper, K. Papadopoulos, R.N. Sudan, S.O. Dean, and E.A. McLean, and J.M. Dawson, Phys. Rev. Lett. 26, 1012 (1971).
2. S.O. Dean, E.A. McLean, J.A. Stamper, and H.R. Griem, Phys. Rev. Lett. 27, 487 (1971).
3. J.A. Stamper, S.O. Dean, and E.A. McLean in Laser Interaction and Related Plasma Phenomena, edited by H. Schwarz and H. Hora (Plenum, New York, 1972), Vol. 2, p. 273.
4. J.A. Stamper, S.H. Gold, S.P. Obenschain, E.A. McLean, and L. Sica, J. Appl. Phys. 52, 6562 (1981).
5. B.H. Ripin, J.A. Stamper, and E.A. McLean, pg. of these proceedings.
6. C. Longmire, pg. of these proceedings.
7. M. Keskinen, pg. of these proceedings.
8. J. Lyon, pg. of these proceedings.
9. J.A. Stamper, S.P. Obenschain, B.H. Ripin, E.A. McLean, J. Grun, and M.J. Herbst, NRL Memorandum Report 5093, June 1983. (AD-129 723)

Appendix: Density Estimate from Refraction

I. Angle of refraction (second harmonic probe)

$$\theta = \int |\nabla n| ds; \quad n \equiv \ln \bar{n}; \quad \bar{n} = \sqrt{1 - n/4n_c}$$

II. Spherical shell ($n/n_c = \exp(-(r-r_0)/L)$)

A. Sagitta Formula

$$d \approx \sqrt{8rs}$$

$$\frac{n}{n_c} \approx \frac{rL\theta}{\sqrt{2rs}} = 4 \sqrt{\frac{L}{2r}} \theta, \quad \text{if } s = L$$

B. Bouguer's Relation ($b = a\bar{n}(a) = r\bar{n}(r) \sin \angle(R, r)$)

$$\theta = \pi - 2b \int_a^\infty \frac{dr}{r \sqrt{r^2 \bar{n}^2(r) - b^2}}$$

$$\frac{n}{n_c} \approx \sqrt{\frac{L}{2a}} \theta, \quad \text{for } \theta \ll 1 \text{ and } L/a, L/r_0, (a-r_0)/r_0 \ll 1$$

$$\text{III. } \frac{n > 10^{17} \text{ cm}^{-3}}{L = 10^{-2} \text{ cm}, r = 1 \text{ cm}} \quad \text{for } \theta > 10^{-2}/25 = 4 \times 10^{-4} \text{ and } n_c = 10^{21} \text{ cm}^{-3},$$

DISTRIBUTION LIST

DEPARTMENT OF DEFENSE

ASSISTANT SECRETARY OF DEFENSE
COMD, CND, CONT 7 INTELL
WASHINGTON, D.C. 20301

DIRECTOR
COMMAND CONTROL TECHNICAL CENTER
PENTAGON RM BE 685
WASHINGTON, D.C. 20301
O1CY ATTN C-650
O1CY ATTN C-312 R. MASON

DIRECTOR
DEFENSE ADVANCED RSCH PROJ AGENCY
ARCHITECT BUILDING
1400 WILSON BLVD.
ARLINGTON, VA. 22209
O1CY ATTN NUCLEAR MONITORING RESEARCH
O1CY ATTN STRATEGIC TECH OFFICE

DEFENSE COMMUNICATION ENGINEER CENTER
1860 WIEHLE AVENUE
RESTON, VA. 22090
O1CY ATTN CODE R410
O1CY ATTN CODE R812

DEFENSE TECHNICAL INFORMATION CENTER
CAMERON STATION
ALEXANDRIA, VA. 22314
O2CY

DIRECTOR
DEFENSE NUCLEAR AGENCY
WASHINGTON, D.C. 20305
O1CY ATTN STVL
O4CY ATTN TITL
O1CY ATTN DBST
O3CY ATTN RAAE

COMMANDER
FIELD COMMAND
DEFENSE NUCLEAR AGENCY
KIRTLAND, AFB, NM 87115
O1CY ATTN FCPR

DIRECTOR
INTERSERVICE NUCLEAR WEAPONS SCHOOL
KIRTLAND AFB, NM 87115
O1CY ATTN DOCUMENT CONTROL

JOINT CHIEFS OF STAFF
WASHINGTON, D.C. 20301
O1CY ATTN J-3 WWMCCS EVALUATION OFFICE

DIRECTOR
JOINT STRAT TCT PLANNING STAFF
OFFUTT AFB
OMAHA, NB 68113
O1CY ATTN JLTH-2
O1CY ATTN JPST C. COETZ

CHIEF
LIVERMORE DIVISION FLD COMMAND DNA
DEPARTMENT OF DEFENSE
LAWRENCE LIVERMORE LABORATORY
P.O. BOX 808
LIVERMORE, CA 94550
O1CY ATTN FCPL

COMMANDANT
NATO SCHOOL (SHAPE)
APO NEW YORK 09172
O1CY ATTN U.S. DOCUMENTS OFFICER

UNDER SECY OF DEF FOR RSCH & ENGRG
DEPARTMENT OF DEFENSE
WASHINGTON, D.C. 20301
O1CY ATTN STRATEGIC & SPACE SYSTEMS (OS)

WWMCCS SYSTEM ENGINEERING ORG
WASHINGTON, D.C. 20305
O1CY ATTN R. CRAWFORD

COMMANDER/DIRECTOR
ATMOSPHERIC SCIENCES LABORATORY
U.S. ARMY ELECTRONICS COMMAND
WHITE SANDS MISSILE RANGE, NM 88002
O1CY ATTN DELAS-EO F. NILES

DIRECTOR
BMD ADVANCED TECH CTR
HUNTSVILLE OFFICE
P.O. BOX 1500
HUNTSVILLE, AL 35807
O1CY ATTN ATC-T MELVIN T. CAPPS
O1CY ATTN ATC-O W. DAVIES
O1CY ATTN ATC-R DON RUSS

PROGRAM MANAGER
BMD PROGRAM OFFICE
5001 EISENHOWER AVENUE
ALEXANDRIA, VA 22333
O1CY ATTN DACS-BMT J. SHEA

CHIEF C-E- SERVICES DIVISION
U.S. ARMY COMMUNICATIONS CMD
PENTAGON RM 1B269
WASHINGTON, D.C. 20310
O1CY ATTN C- E-SERVICES DIVISION

COMMANDER
FRADCOM TECHNICAL SUPPORT ACTIVITY
DEPARTMENT OF THE ARMY
FORT MONMOUTH, N.J. 07703
O1CY ATTN DRSEL-NL-RD H. BENNET
O1CY ATTN DRSEL-PL-ENV H. BOMEKE
O1CY ATTN J.E. QUIGLEY

COMMANDER
U.S. ARMY COMM-ELEC ENGRG INSTAL AGY
FT. HUACHUCA, AZ 85613
O1CY ATTN CCC-EMEO GEORGE LANE

COMMANDER
U.S. ARMY FOREIGN SCIENCE & TECH CTR
220 7TH STREET, NE
CHARLOTTESVILLE, VA 22901
O1CY ATTN DRXST-SD

COMMANDER
U.S. ARMY MATERIAL DEV & READINESS CMD
5001 EISENHOWER AVENUE
ALEXANDRIA, VA 22333
O1CY ATTN DRCLDC J.A. BENDER

COMMANDER
U.S. ARMY NUCLEAR AND CHEMICAL AGENCY
7500 BACKLICK ROAD
BLDG 2073
SPRINGFIELD, VA 22150
O1CY ATTN LIBRARY

DIRECTOR
U.S. ARMY BALLISTIC RESEARCH LABORATORY
ABERDEEN PROVING GROUND, MD 21005
O1CY ATTN TECH LIBRARY EDWARD BAICY

COMMANDER
U.S. ARMY SATCOM AGENCY
FT. MONMOUTH, NJ 07703
O1CY ATTN DOCUMENT CONTROL

COMMANDER
U.S. ARMY MISSILE INTELLIGENCE AGENCY
REDSTONE ARSENAL, AL 35809
O1CY ATTN JIM GAMBLE

DIRECTOR
U.S. ARMY TRADOC SYSTEMS ANALYSIS ACTIVITY
WHITE SANDS MISSILE RANGE, NM 88002
O1CY ATTN ATAA-SA
O1CY ATTN TCC/F. PAYAN JR.
O1CY ATTN ATTA-TAC LTC J. HESSE

COMMANDER
NAVAL ELECTRONIC SYSTEMS COMMAND
WASHINGTON, D.C. 20360
O1CY ATTN NAVALEX 034 T. HUGHES
O1CY ATTN PME 117
O1CY ATTN PME 117-T
O1CY ATTN CODE 5011

COMMANDING OFFICER
NAVAL INTELLIGENCE SUPPORT CTR
4301 SUITLAND ROAD, BLDG. 5
WASHINGTON, D.C. 20390
O1CY ATTN MR. DUBBIN STIC 12
O1CY ATTN NISC-50
O1CY ATTN CODE 5404 J. GALET

COMMANDER
NAVAL OCEAN SYSTEMS CENTER
SAN DIEGO, CA 92152
O1CY ATTN J. FERGUSON

NAVAL RESEARCH LABORATORY
WASHINGTON, DC 20375

01CY ATTN CODE 4700 S.L. OSSAKOW
26 CYS IF UNCLASS, 1 CY IF CLASS
01CY ATTN CODE 4701 I. VITKOVITSKY
01CY ATTN CODE 4780 J. Huba (10
CYS IF UNCLASS, 1 CY IF CLASS)
01CY ATTN CODE 7500
01CY ATTN CODE 7550
01CY ATTN CODE 7580
01CY ATTN CODE 7551
01CY ATTN CODE 7555
01CY ATTN CODE 4730 E. MCLEAN
01CY ATTN CODE 4108
01CY ATTN CODE 4730 B. RIPIN
20CY ATTN CODE 2628
100CY ATTN CODE 4730

COMMANDER
NAVAL SEA SYSTEMS COMMAND
WASHINGTON, DC 20362
01CY ATTN CAPT R. PITKIN

COMMANDER
NAVAL SPACE SURVEILLANCE SYSTEM
DHALGREN, VA 22448
01CY ATTN CAPT J.H. BURTON

OFFICER-IN-CHARGE
NAVAL SURFACE WEAPONS CENTER
WHITE OAK, SILVER SPRING, MD 20910
01CY ATTN CODE F31

DIRECTOR
STRATEGIC SYSTEMS PROJECT OFFICE
DEPARTMENT OF THE NAVY
WASHINGTON, DC 20376
01CY ATTN NSP-2141
01CY ATTN NSSP-2722 FRED WIMBERLY

COMMANDER
NAVAL SURFACE WEAPONS CENTER
DAHLGREN LABORATORY
DAHLGREN, VA 22448
01CY ATTN CODE DF-14 R. BUTLER

OFFICE OF NAVAL RESEARCH
ARLINGTON, VA 22217

01CY ATTN CODE 465
01CY ATTN CODE 461
01CY ATTN CODE 402
01CY ATTN CODE 420
01CY ATTN CODE 421

COMMANDER
AEROSPACE DEFENSE COMMAND/DC
DEPARTMENT OF THE AIR FORCE
ENT AFB, CO 90912
01CY ATTN DC MR. LONG

COMMANDER AEROSPACE DEFENSE COMMAND/XPD
DEPARTMENT OF THE AIR FORCE
ENT AFB, CO 80912
01CY ATTN XPDQQ
01CY ATTN XP

AIR FORCE GEOPHYSICS LABORATORY
HANSCOM AFB, MA 01731
01CY ATTN OPR HAROLD GARDNER
01CY ATTN LKB KENNETH S.W. CHAMPION
01CY ATTN OPR ALVA T. STAIR
01CY ATTN PHD JURGEN BUCHAU
01CY ATTN PHD JOHN P. MULLEN

AF WEAPONS LABORATORY
KIRTLAND AFB, NM 87117
01CY ATTN SUL
01CY ATTN CA ARTHUR H. GUENTHER
01CY ATTN NTYCE LT. G. KRAJEI

AFTAC
PATRICK AFB, FL 32925
01CY ATTN IF/MAJ WILEY
01CY ATTN TN

AIR FORCE AVIONICS LABORATORY
WRIGHT-PATTERSON AFB, OH 45433
01CY ATTN AAD WADE HUNT
01CY ATTN AAD ALLEN JOHNSON

DEPUTY CHIEF OF STAFF
RESEARCH, DEVELOPMENT, & ACQ
DEPARTMENT OF THE AIR FORCE
WASHINGTON, DC 20030
01CY ATTN AFRDQ

HEADQUARTERS
ELECTRONIC SYSTEMS DIVISION
DEPARTMENT OF THE AIR FORCE
HANSCOM AFB, MA 01731
01CY ATTN J. DEAS

HEADQUARTERS
ELECTRONIC SYSTEMS DIVISION/YSEA
DEPARTMENT OF THE AIR FORCE
HANSCOM AFB, MA 01732
01CY ATTN YSEA

HEADQUARTERS
ELECTRONIC SYSTEMS DIVISION/DC
DEPARTMENT OF THE AIR FORCE
HANSCOM AFB, MA 01731
O1CY ATTN DCKC MAJ J.C. CLARK

COMMANDER
FOREIGN TECHNOLOGY DIVISION, AFSC
WRIGHT-PATTERSON AFB, OH 45433
O1CY ATTN NICD LIBRARY
O1CY ATTN ETD B. BALLARD

COMMANDER
ROME AIR DEVELOPMENT CENTER, AFSC
GRIFFISS AFB, NY 13441
O1CY ATTN DOC LIBRARY/ISLD
O1CY ATTN OCSE V. COYNE

SAMSO/SZ
POST OFFICE BOX 92960
WORLDWAY POSTAL CENTER
LOS ANGELES, CA 90009
(SPACE DEFENSE SYSTEMS)
O1CY ATTN SZJ

STRATEGIC AIR COMMAND/XPFS
OFFUTT AFB, NE 68113
O1CY ATTN ADWATE MAJ BRUCE BAUER
O1CY ATTN NRT
O1CY ATTN DOK CHIEF SCIENTIST

SAMSC/SK
P.O. BOX 92960
WORLDWAY POSTAL CENTER
LOS ANGELES, CA 90009
O1CY ATTN SKA (SPACE COMM SYSTEMS)
M. CLAVIN

SAMSO/MM
NORTON AFB, CA 92409
(MINUTEMAN)
O1CY ATTN MMNL

COMMANDER
ROME AIR DEVELOPMENT CENTER, AFSC
HANSCOM AFB, MA 01731
O1CY ATTN EEP A. LORENTZEN

DEPARTMENT OF ENERGY
LIBRARY ROOM G-042
WASHINGTON, D.C. 20545
O1CY ATTN DOC CON FOR A. LABOWITZ

DEPARTMENT OF ENERGY
ALBUQUERQUE OPERATIONS OFFICE
P.O. BOX 5400
ALBUQUERQUE, NM 87115
O1CY ATTN DOC CON FOR D. SHERWOOD

EG&G, INC.
LOS ALAMOS DIVISION
P.O. BOX 809
LOS ALAMOS, NM 85544
O1CY ATTN DOC CON FOR J. BREEDLOVE

UNIVERSITY OF CALIFORNIA
LAWRENCE LIVERMORE LABORATORY
P.O. BOX 808
LIVERMORE, CA 94550
O1CY ATTN DOC CON FOR TECH INFO DEPT
O1CY ATTN DOC CON FOR L-389 R. OTT
O1CY ATTN DOC CON FOR L-31 R. HAGER
O1CY ATTN DOC CON FOR L-46 F. SEWARD

LOS ALAMOS NATIONAL LABORATORY
P.O. BOX 1663
LOS ALAMOS, NM 87545
O1CY ATTN DOC CON FOR J. WOLCOTT
O1CY ATTN DOC CON FOR R.F. TASCHEK
O1CY ATTN DOC CON FOR E. JONES
O1CY ATTN DOC CON FOR J. MALIK
O1CY ATTN DOC CON FOR R. JEFFRIES
O1CY ATTN DOC CON FOR J. ZINN
O1CY ATTN DOC CON FOR P. KEATON
O1CY ATTN DOC CON FOR D. WESTERVELT
O1CY ATTN D. SAPPENFIELD

SANDIA LABORATORIES
P.O. BOX 5800
ALBUQUERQUE, NM 87115
O1CY ATTN DOC CON FOR W. BROWN
O1CY ATTN DOC CON FOR A. THORNBROUGH
O1CY ATTN DOC CON FOR T. WRIGHT
O1CY ATTN DOC CON FOR D. DAHLGREN
O1CY ATTN DOC CON FOR 3141
O1CY ATTN DOC CON FOR SPACE PROJECT DIV

SANDIA LABORATORIES
LIVERMORE LABORATORY
P.O. BOX 969
LIVERMORE, CA 94550
O1CY ATTN DOC CON FOR B. MURPHEY
O1CY ATTN DOC CON FOR T. COOK

OFFICE OF MILITARY APPLICATION
DEPARTMENT OF ENERGY
WASHINGTON, D.C. 20545
O1CY ATTN DOC CON DR. YO SONG

OTHER GOVERNMENT

DEPARTMENT OF COMMERCE
NATIONAL BUREAU OF STANDARDS
WASHINGTON, D.C. 20234
OICY (ALL CORRES: ATTN SEC OFFICER FOR)

INSTITUTE FOR TELECOM SCIENCES
NATIONAL TELECOMMUNICATIONS & INFO ADMIN
BOULDER, CO 80303
OICY ATTN A. JEAN (UNCLASS ONLY)
OICY ATTN W. UTLAUT
OICY ATTN D. CROMBIE
OICY ATTN L. BERRY

NATIONAL OCEANIC & ATMOSPHERIC ADMIN
ENVIRONMENTAL RESEARCH LABORATORIES
DEPARTMENT OF COMMERCE
BOULDER, CO 80302
OICY ATTN R. GRUBB
OICY ATTN AERONOMY LAB G. REID

DEPARTMENT OF DEFENSE CONTRACTORS

AEROSPACE CORPORATION
P.O. BOX 92957
LOS ANGELES, CA 90009
OICY ATTN I. GARFUNKEL
OICY ATTN T. SALMI
OICY ATTN V. JOSEPHSON
OICY ATTN S. BOWER
OICY ATTN D. OLSEN

ANALYTICAL SYSTEMS ENGINEERING CORP
5 OLD CONCORD ROAD
BURLINGTON, MA 01803
OICY ATTN RADIO SCIENCES

AUSTIN RESEARCH ASSOC., INC.
1901 RUTLAND DRIVE
AUSTIN, TX 78758
OICY ATTN L. SLOAN
OICY ATTN R. THOMPSON

BERKELEY RESEARCH ASSOCIATES, INC.
P.O. BOX 983
BERKELEY, CA 94701
OICY ATTN J. WORKMAN
OICY ATTN C. PRETTIE
OICY ATTN S. BRECHT

BOEING COMPANY, THE
P.O. BOX 3707
SEATTLE, WA 98124
OICY ATTN G. KEISTER
OICY ATTN D. MURRAY
OICY ATTN G. HALL
OICY ATTN J. KENNEY

CHARLES STARK DRAPER LABORATORY, INC.
555 TECHNOLOGY SQUARE
CAMBRIDGE, MA 02139
OICY ATTN D.B. COX
OICY ATTN J.P. GILMORE

COMSAT LABORATORIES
LINTHICUM ROAD
CLARKSBURG, MD 20734
OICY ATTN G. HYDE

CORNELL UNIVERSITY
DEPARTMENT OF ELECTRICAL ENGINEERING
ITHACA, NY 14850
OICY ATTN D.T. FARLEY, JR.

ELECTROSPACE SYSTEMS, INC.
BOX 1359
RICHARDSON, TX 75080
OICY ATTN H. LOGSTON
OICY ATTN SECURITY (PAUL PHILLIPS)

EOS TECHNOLOGIES, INC.
606 Wilshire Blvd.
Santa Monica, Calif 90401
OICY ATTN C.B. GABBARD

ESL, INC.
495 JAVA DRIVE
SUNNYVALE, CA 94086
OICY ATTN J. ROBERTS
OICY ATTN JAMES MARSHALL

GENERAL ELECTRIC COMPANY
SPACE DIVISION
VALLEY FORGE SPACE CENTER
GODDARD BLVD KING OF PRUSSIA
P.O. BOX 8555
PHILADELPHIA, PA 19101
OICY ATTN M.H. BORTNER SPACE SCI LAB

GENERAL ELECTRIC COMPANY
P.O. BOX 1122
SYRACUSE, NY 13201
OICY ATTN F. REIBERT

GENERAL ELECTRIC TECH SERVICES CO., INC.
HMES
COURT STREET
SYRACUSE, NY 13201
OICV ATTN G. MILLMAN

GEOPHYSICAL INSTITUTE
UNIVERSITY OF ALASKA
FAIRBANKS, AK 99701
(ALL CLASS ATTN: SECURITY OFFICER)
OICV ATTN T.N. DAVIS (UNCLASS ONLY)
OICV ATTN TECHNICAL LIBRARY
OICV ATTN NEAL BROWN (UNCLASS ONLY)

GTE SYLVANIA, INC.
ELECTRONICS SYSTEMS GRP-EASTERN OIV
77 A STREET
NEEDHAM, MA 02194
OICV ATTN OICK STEINHOF

HSS, INC.
2 ALFREO CIRCLE
BEDFORD, MA 01730
OICV ATTN DONALD HANSEN

ILLINOIS, UNIVERSITY OF
107 COBLE HALL
150 OAVENPORT HOUSE
CHAMPAIGN, IL 61820
(ALL CORRES ATTN DAN MCCLELLAND)
OICV ATTN K. YEH

INSTITUTE FOR DEFENSE ANALYSES
1801 NO. BEAUREGARD STREET
ALEXANDRIA, VA 22311
OICV ATTN J.M. ASIN
OICV ATTN ERNEST BAUER
OICV ATTN HANS WOLFARD
OICV ATTN JOEL BENGSTON

INTL TEL & TELEGRAPH CORPORATION
500 WASHINGTON AVENUE
NUTLEY, NJ 07110
OICV ATTN TECHNICAL LIBRARY

JAYCOR
11011 TORREYANA ROAD
P.O. BOX 85154
SAN DIEGO, CA 92138
OICV ATTN J.L. SPERLING

JOHNS HOPKINS UNIVERSITY
APPLIED PHYSICS LABORATORY
JOHNS HOPKINS ROAD
LAUREL, MD 20810
OICV ATTN DOCUMENT LIBRARIAN
OICV ATTN THOMAS POTEIRA
OICV ATTN JOHN OASSOULAS

KAMAN SCIENCES CORP
P.O. BOX 7463
COLORADO SPRINGS, CO 80933
OICV ATTN T. MEAGHER

KAMAN TEMPO-CENTER FOR ADVANCED STUOIES
916 STATE STREET (P.O. DRAWER QQ)
SANTA BARBARA, CA 93102
OICV ATTN DASIAC
OICV ATTN WARREN S. KNAPP
OICV ATTN WILLIAM MCNAMARA
OICV ATTN B. GAMBILL

LINKABIT CORP
10453 ROSELLE
SAN DIEGO, CA 92121
OICV ATTN IRWIN JACOBS

LOCKHEED MISSILES & SPACE CO., INC
P.O. BOX 504
SUNNYVALE, CA 94088
OICV ATTN DEPT 60-12
OICV ATTN D.R. CHURCHILL

LOCKHEED MISSILES & SPACE CO., INC.
3251 HANOVER STREET
PALO ALTO, CA 94304
OICV ATTN MARTIN WALT DEPT 52-12
OICV ATTN W.L. IMIOF DEPT 52-12
OICV ATTN RICHARD G. JOHNSON OEPT 52-12
OICV ATTN J.B. CLADIS OEPT 52-12

MARTIN MARIETTA CORP
ORLANDO DIVISION
P.O. BOX 5837
ORLANDO, FL 32805
OICV ATTN R. HEFFNER

M.I.T. LINCOLN LABORATORY
P.O. BOX 73
LEXINGTON, MA 02173
OICV ATTN DAVID M. TOWLE
OICV ATTN L. LOUGHLIN
OICV ATTN O. CLARK

MCDONNELL DOUGLAS CORPORATION
5301 BOLSA AVENUE
HUNTINGTON BEACH, CA 92647
O1CY ATTN N. HARRIS
O1CY ATTN J. MOULE
O1CY ATTN GEORGE MROZ
O1CY ATTN W. OLSON
O1CY ATTN R.W. HALPRIN
O1CY ATTN TECHNICAL LIBRARY SERVICES

MISSION RESEARCH CORPORATION
735 STATE STREET
SANTA BARBARA, CA 93101
O1CY ATTN P. FISCHER
O1CY ATTN W.F. GREVIER
O1CY ATTN STEVEN L. GUTSCHE
O1CY ATTN R. BOGUSCH
O1CY ATTN R. HENDRICK
O1CY ATTN RALPH KILB
O1CY ATTN DAVE SOWLE
O1CY ATTN F. FAJEN
O1CY ATTN M. SCHEIBE
O1CY ATTN CONRAD L. LONGMIRE
O1CY ATTN B. WHITE

MISSION RESEARCH CORPORATION
1720 RANDOLPH ROAD, SE
ALBUQUERQUE, NM 87106
O1CY ATTN R. STELLINGWERF
O1CY ATTN M. ALME
O1CY ATTN L. WRIGHT

MITRE CORPORATION, THE
P.O. BOX 208
BEDFORD, MA 01730
O1CY ATTN JOHN MORGANSTERN
O1CY ATTN G. HARDING
O1CY ATTN G.E. CALLAHAN

MITRE CORPORATION
WESTGATE RESEARCH PARK
1820 DOLLY MADISON BLVD.
MCLEAN, VA 22101
O1CY ATTN W. HALL
O1CY ATTN W. FOSTER

PACIFIC-SIERRA RESEARCH CORP.
12340 SANTA MONICA BLVD.
LOS ANGELES, CA 90025
O1CY ATTN E.C. FIELD, JR.

PENNSYLVANIA STATE UNIVERSITY
IONOSPHERE RESEARCH LAB
318 ELECTRICAL ENGINEERING EAST
UNIVERSITY PARK, PA 16802
(NO CLASS. TO THIS ADDRESS)
O1CY ATTN IONOSPHERIC RESEARCH LAB

PHOTOMETRICS, INC.
4 ARROW DRIVE
WOBURN, MA 01801
O1CY ATTN IRVING L. KOFSKY

PHYSICAL DYNAMICS, INC.
P.O. BOX 3027
BELLEVUE, WA 98009
O1CY ATTN E.J. FREMOW

PHYSICAL DYNAMICS, INC.
P.O. BOX 10367
OAKLAND, CA 94610
O1CY ATTN A. THOMSON

R&D ASSOCIATES
P.O. BOX 9695
MARINA DEL REY, CA 90291
O1CY ATTN FORREST GILMORE
O1CY ATTN WILLIAM B. WRIGHT, JR.
O1CY ATTN ROBERT F. LELEVIER
O1CY ATTN WILLIAM J. KARZAS
O1CY ATTN H. ORY
O1CY ATTN C. MAGDONALD
O1CY ATTN R. TURCO
O1CY ATTN L. DeRADD

RAND CORPORATION, THE
1700 MAIN STREET
SANTA MONICA, CA 90406
O1CY ATTN CULLEN CRAIN
O1CY ATTN ED BEDROZIAN

RAYTHEON COMPANY
528 BOSTON POST ROAD
SUDBURY, MA 01776
O1CY ATTN BARBARA ADAMS

SCIENCE APPLICATIONS, INC.
P.O. BOX 2351
LA JOLLA, CA 92038

OICY ATTN LEWIS M. LINSON
OICY ATTN DANIEL A. HANLIN
OICY ATTN E. FRIEMAN
OICY ATTN E.A. STRAKER
OICY ATTN CURTIS A. SMITH
OICY ATTN JACK MCDOUGALL

SCIENCE APPLICATIONS, INC
1710 GOODRIDGE DR.
MCLEAN, VA 22102
ATTN: J. COCKAYNE

SRI INTERNATIONAL
333 RAVENSWOOD AVENUE
MENLO PARK, CA 94025
OICY ATTN DONALD NEILSON
OICY ATTN ALAN BURNS
OICY ATTN G. SMITH
OICY ATTN R. TSUNODA
OICY ATTN DAVID A. JOHNSON
OICY ATTN WALTER G. CHESNUT
OICY ATTN CHARLES L. RINO
OICY ATTN WALTER JAYE
OICY ATTN J. VICKREY
OICY ATTN RAY L. LEADABRAND
OICY ATTN G. CARPENTER
OICY ATTN G. PRICE
OICY ATTN R. LIVINGSTON
OICY ATTN V. GONZALES
OICY ATTN D. MCDANIEL

TECHNOLOGY INTERNATIONAL CORP
75 WIGGINS AVENUE
BEDFORD, MA 01730
OICY ATTN W.P. BOQUIST

TOYON RESEARCH CO.
P.O. Box 6890
SANTA BARBARA, CA 93111
OICY ATTN JOHN ISE, JR.
OICY ATTN JOEL GARBARINO

TRW DEFENSE & SPACE SYS GROUP
ONE SPACE PARK
REDONDO BEACH, CA 90278
OICY ATTN R. K. PLEBUCH
OICY ATTN S. ALTSCHULER
OICY ATTN D. DEE
OICY ATTN D/ STOCKWELL
SNIF/1575

VISIDYNE
SOUTH BEDFORD STREET
BURLINGTON, MASS 01803
OICY ATTN W. REIDY
OICY ATTN J. CARPENTER
OICY ATTN C. HUMPHREY

**DAT
FILM**